MICROCOPY RESOLUTION TEST CHART

NATIONAL BUREAU OF STANDARDS-1963 A

OFFICE OF NAVAL RESEARCH

Contract N00014-76-C-0408

Project NR 092-555

Technical Report No. 26

FRACTURE TOUGHNESS OF POLYBUTADIENE

AT CRYOGENIC TEMPERATURES

by

R. P. Burford

Institute of Polymer Science
The University of Akron
Akron, Ohio 44325

April, 1983

Reproduction in whole or in part is permitted

for any purpose of the United States Government

Approved for Public Release; Distribution Unrestricted

REPORT DOCUMENTATION PAGE		READ INSTRUCTIONS BEFORE COMPLETING FORM
1. REPORT NUMBER Technical Report No. 26	2. GOVT ACCESSION NO. AD H126 999	3. RECIPIENT'S CATALOG NUMBER
4. TITLE (and Subtitle) Fracture Toughness of Polybutadiene at Cryogenic Temperatures		5. TYPE OF REPORT & PERIOD COVERED Technical Report
		6. PERFORMING ORG. REPORT NUMBER
7. AUTHOR(s) R. P. Burford		8. CONTRACT OR GRANT NUMBER(s) N00014-76-C-0408
9. PERFORMING ORGANIZATION NAME AND ADDRESS Institute of Polymer Science The University of Akron Akron, Ohio 44325		10. PROGRAM ELEMENT, PROJECT, TASK AREA & WORK UNIT NUMBERS NR 092-555
11. CONTROLLING OFFICE NAME AND ADDRESS Office of Naval Research Power Program Arlington, VA 22217		12. REPORT DATE April, 1983
		13. NUMBER OF PAGES 35
14. MONITORING AGENCY NAME & ADDRESS(if different from Controlling Office)		15. SECURITY CLASS. (of this report) Unclassified
		15a. DECLASSIFICATION/DOWNGRADING SCHEDULE

16. DISTRIBUTION STATEMENT (of this Report)

~~According to attached distribution list.~~
Approved for public release; distribution unrestricted.

17. DISTRIBUTION STATEMENT (of the abstract entered in Block 20, if different from Report)

18. SUPPLEMENTARY NOTES

Submitted for publication in: Journal of Materials Science

19. KEY WORDS (Continue on reverse side if necessary and identify by block number)

Crack propagation, Crazing, Crosslinked, Double-Torsion, Fracture, Polybutadiene, Rubber, Strength, Toughness

20. ABSTRACT (Continue on reverse side if necessary and identify by block number)

An estimate of fracture toughness of crosslinked polybutadiene rubber at -180°C has been made using the double torsion method. By using suitable specimen dimensions and strain rates, controlled crack propagation can be achieved, together with a constant compliance to crack length ratio. Strain energy release rates for this polymer, crosslinked with either dicumyl peroxide or sulphur, were found to be an order of magnitude higher than for linear, glassy thermoplastics. Crazing is considered to contribute to the high toughness observed.

DD FORM 1473 EDITION OF 1 NOV 65 IS OBSOLETE
1 JAN 73
S/N 0102-LF-014-6601

S/N 0102- LF- 014- 6601

1. Introduction

At room temperature crosslinked elastomers are widely used as tough engineering materials because of their high elongation at break, coupled with unique elastic recovery properties. When chilled below its glass transition, rubber loses much of its toughness, as indicated by brittle, shattering behaviour when impacted at liquid nitrogen (-180°C) temperatures. This embrittlement process has been commercially exploited in cryogenic comminution [1-3]; fine powders can be produced with low energy expenditure. Despite widespread recognition of this transformation in behaviour, no attempts to measure Mode 1 fracture toughness at cryogenic temperatures have previously been recorded for elastomers.

Fracture toughness (K), and energy release rates (G) have been measured for both ductile and brittle polymers using a variety of configurations [4]. From this compilation it is noted that for polybutadiene rubbers in tearing Mode III, G_{Ic} ranges from threshold values of about 20 J m^{-2} (highly swollen and at elevated temperatures) [5] to a maximum of approximately 1 [5] to 3 kJ m^{-2} [6]. As crosslink density increases (i.e. Mc decreases), threshold fracture energy decreases [5].

For a linear thermoplastic with Tg above 20°C, many methods are available for convenient measurement of K and G; no serious constraints upon specimen geometry exist, and crack length parameter a can be readily measured in situ. For many temperatures and strain rates, PMMA's of varying molecular weight show a quite narrow range of toughness values, with G_{Ic} ranging from 100 to 1000 Jm^{-2} and K_{Ic} between 1 and 3 MNm$^{-3/2}$ [4,7,8]. Unfilled thermosetting resins including epoxy and unsaturated polyester resins also show similar toughness

values [4]; tougher polymers include higher impact engineering grades
(for example, ABS and polycarbonate) for which crack bluntening con-
tributes to G_{Ic} values of around 3 to 20 kJm^{-2} and filled composites
with G_{Ic} often greater than 10 kJm^{-2} [4].

For materials including glass [9], alumina [10,11] and rigid thermo-
plastics (PMMA [8,12,13], polycarbonate [14] and epoxy resins [15,19]
a convenient method for determining fracture energy and toughness is
the double torsion technique.   Uncertainty exists as to whether failure
is of Mode III type (as crack growth is in the x direction) or Mode I
(plausible from crack propagation being nearly parallel to z direction)
but Jayatilaka [20] considers despite the good agreement with G_{Ic} data
obtained by other methods that the issue is still unresolved.

In practice the double torsion method is potentially ideal for
cryogenic fracture toughness measurement.   Two major advantages exist:
G_{Ic} can be measured independent of crack length, thus reducing much
tedious effort and secondly, the compact compression mode of load
application is easily adapted to incorporate unusual environments.
Alternative crack opening displacement (COD) methods would entail
much more elaborate and less direct techniques.

In this study polybutadiene rubbers crosslinked with either dicumyl
peroxide or sulphur were fractured in liquid nitrogen using the double
torsion method.   From a structural viewpoint, these materials are more
readily characterized compared with crosslinked epoxy polymers.   The
latter, essentially multicomponent materials, are not easily defined
because linear polymerisation and other uncontrolled side reactions
occur concurrently with curing.

Elastomers are initially well above Tg and so thermodynamically
at equilibrium.   Molecular weights and chain architecture can be

readily determined. Crosslinking is in the absence of concommittent linear polymerization, and the degree of crosslinking in essentially homogeneous material can be accurately monitored and controlled. Hence it should be possible for the effects of Mc upon fracture energy to be unambiguously determined.

In this paper the fracture energy of high-cis-polybutadiene is measured when immersed in liquid nitrogen. Details concerning the experimental procedure and its validity are included, together with a brief description of fracture morphology.

2.   Experimental Procedure

2.1 Elastomers

In this study the base polymer was "cis-4 1203" polybutadiene (BR) provided by Phillips Petroleum Co., Bartlesville. Typically this polymer has a 92% cis content, a Mw of about 380,000 and a polydispersity of 2.1 [21].

"Dicup R" dicumyl peroxide (Hercules Chemical Co., Wilmington) was dispersed into thin BR crepe, milled and massed. From cure rheometer traces, vulcanization at 150°C for 2h was chosen. Sheets 3 to 5 mm in thickness were made between polyester film, using suitable plate dies. Crosslink densities were then determined by swelling in n-heptane, using the Flory-Rehner equation [22] and constants from Kraus [23]. Details of this group of polymers are summarized in Table 1. Increase in Monsanto torque has been listed at an arbitrary 60 minutes cure time to reflect modulus changes at each level of peroxide.

Sulphur crosslinked BR samples were prepared using basically the formulation of Henry and Gent [24]. The rubber was premixed at 60 rpm in a Brabender RE-6 instrument for 2 minutes, followed by addition of zinc oxide, stearic acid, TBBS accelerator and sulphur, each at 1 min

intervals. After a total mix time of 6 min, the off-white polymer was passed 10 times on a Farrell mill, before massing and vulcanization. Details of samples at three sulphur levels (chosen to centre about a typical, commercial value) are provided in Table II.

TABLE I. Peroxide crosslinked BR - formulation and properties

Dicup Level - parts/100 rubber	Change in Monsanto Torque after 60 mins (lb/inch)	M_c (using $=0.32+.57V_R$)	SG
0.05	29	61,300	-
0.20	40	6,200	0.90
0.40	55	3,800	0.91
0.60	64	3,300	0.91
1.00	75	3,000	-

TABLE II. Sulphur-cured BR - formulation and properties

Sample Code. (Based on 100 parts hydrocarbon)	Sulphur	Change in Monsanto Torque after 60 mins. (lb inch)	M_c	SG
A	1.0	38	4,900	0.95
B	1.5	50	3,700	0.95
C	2.0	57	3,200	0.94

Strips approximately 13 mm wide and 60 mm long were guillotined for flexural modulus determination at -180°C. Other samples, from 25 to 30 mm wide and from 80 to 100 mm long were prepared for double torsion testing, as described below.

2.1 Double torsion test method

Established procedures (for example, described in refs. 9,10) were varied in that a steel "U" frame was used instead of rollers to support the test piece and the load was applied via a 6.5 mm diameter ball bearing attached via a slender probe to the descending Instron crosshead. Cryogenic experiments were conducted with specimens resting in liquid nitrogen, contained in a flat bottomed aluminium bowl, separated from the compression cell by a 12.5 mm thick PVC/gypsum insulating sheet. This assembly was shown by prior compression trials not to yield significantly under the load range of interest (i.e. up to about 1 KN). The double torsion test apparatus is illustrated in Fig. 1.

Fracture toughness data were obtained in the following manner. Each rubber specimen had a crack guidance groove inserted using a jewellers saw and then prenotched with a sharp, lubricated blade. A "sandwich" of the test-piece clamped between 1 mm thick steel plates (to prevent distortion during cooling) was immersed in liquid nitrogen for about 5 min. The then "liberated" test-piece was held temporarily on the U frame using a small weight. Once the bearing began to deform the test-piece at a controlled crosshead speed, the positioning weight was removed. Using suitable crosshead speeds and specimen dimensions, the load recorded will increase and then plateau.

Often a fine "saw-tooth" trace is obtained, reflecting at a microscopic level crack initiation and arrest; the difference in load is normally small and unimportant when approximate G_{Ic} values are being considered. Care needs to be taken to ensure that the test-piece deforms in the correct manner; plate hinging can arise when the guidance channel is too deep, and trouser tear mode operates when the load is not evenly distributed onto the two "tines" of the test specimen.

Dimensions of the cold, fractured test-piece are then taken, and G_{Ic} is determined from value of constant load, P, specimen dimensions ℓ, D, B, B_c, and modulus G (estimated by 3 point flexing at -180°C, in separate experiments), using equation 1, where constants correspond to those used by Williams (25).

$$G_{Ic} = \frac{3P^2\ell^2}{2D^2B_cB^3G} \qquad (1)$$

In most cases duplicate measurements of G_{Ic} were obtained. Crosshead speeds ranging from 0.5 mm min^{-1} to 50 mm min^{-1} were employed.

2.3 Morphology of fracture surfaces

High resolution examination of fracture morphology during and just after testing was impractical. Macrographs were obtained of fractured specimens in both the liquid nitrogen and in the cold gaseous environment just above the liquid surface. Subsequently test pieces were equilibrated at 20°C, gold coated and examined both optically and by SEM (using a JEOL SM2 instrument).

3. Verification of the Test Procedure

As indicated by Marshall and Williams (8,25), a necessary condition for legitimate results is that compliance C must be proportional to crack length a. Calibration can be undertaken to show that

$$C = \frac{K(1+\nu)}{E} a + C_0$$

where $\quad$ C $\quad = \quad$ compliance at crack length

$\qquad C_0 \quad = \quad$ compliance at crack length $a = 0$

$\qquad$ K $\quad = \quad$ constant incorporating specimen dimensions

$\qquad$ E $\quad = \quad$ tensile modulus

and $\quad \nu \quad = \quad$ Poisson's ratio

Where a load versus deflection trace takes the form shown in Fig. 2, and where subsequent examination of the fracture surface reveals evenly spaced crack arrest lines (for example, Fig. 3), the conditions of proportidnality between C and a are met.

4. Results and Discussion

4.1 Load versus displacement (or time) traces.

Before examining chilled rubber samples, PMMA test pieces of varying dimensions were tested at 20°C using crosshead speeds ranging from 0.5 mm min^{-1} to 100 mm min^{-1}. This was undertaken to check that G_{Ic} values consistant with those already published were obtained, and also to choose convenient conditions which would be suitable for the cryogenic studies. From Fig. 4 it can be seen that toughness increases as strain rate increases for PMMA at 20°C, in much the same way as indicated by Williams and Hodgkinson (Fig. 2 in [27]). Although test specimen thickness, channel depth and length of starter notch were varied, the relatively narrow range of values shown in Fig. 4 indicate that substantial departures in fracture mechanism are absent. In essence, results including fracture morphology agreed closely with those of Hakeem and Phillips [13].

From these preliminary studies, rubber specimens were prepared with dimensions of B typically 3 to 4 mm, B_c 1-2 mm (with channel width being about 1 mm) ℓ was generally fixed at about 12 mm and D ranged from 14 to 20 mm (all dimensions are of rubber at cryogenic temperatures). Occasionally the channel was replaced by a sharp lengthwise incision, again to give B_c about 1.5 mm, but this procedure provided no advantage over the sawn channel method. Finally, starter notches of varying length were tested, but as a steady load was only obtained after the crack had grown substantially, no sensitivity to notch length was

observed.   Unduly long starter notches were avoided as this merely
encouraged specimen warpage during cooling and thus caused experimental
difficulties.

With rubber specimens very deep channels had also to be avoided, as
this led to "hinging", an inappropriate mode of deformation.   It was
found that slower crosshead speeds (≤ 5 mm min^{-1}) gave controlled crack
propagation; a slip-stick trace was often obtained, as shown for
"Cis 4" BR cured with 1 phr sulphur in Fig. 5.   As differences
between crack initiation load P_i and arrest load P_a were generally
small (less than 5%), for the purposes of estimating G for internal
comparison an average can be taken.

In some experiments a smoother trace was obtained (for example
Fig. 6).   This suggests that the mode of failure is changing slightly,
but the emphasis here is to compare the magnitude of G with compound
variables and so discussion on this point will come later.   It is
noted that these two load versus displacement traces correspond to
those shown in Fig. 12 (d) and (f) of Scott et al [19].   However,
one would not expect to see major changes in fracture mechanism in
our case, as temperature and polymer type are fixed.   Those traces from
which G data are presented as "legitimate" also include those correspond-
ing to Figs. 12 (c) and occasionally (g) [19].

When higher crosshead speeds (typically 50 mm min^{-1}) are used,
fracture often occurs before stable crack propagation.   In these
circumstances, a load versus time trace of the type shown in Fig. 7
is obtained.   Maximum loads sustained by specimens in these circumstances were
thus recorded, and in principle corresponding G_{Ic} values can be calculated.
However, these generally low (≤ 5 kJm^{-2}) results are invalid as no stable
crack growth has occurred.

4.2   Fracture Energy Versus Compound Variables

4.2.1 Peroxide cured polymer

The effect of crosslink density (reflected by M_c) upon G_{Ic} is shown in Fig. 8.   It can be seen that there is little sensitivity with G_{Ic} remaining high even at high crosslink densities.   This would suggest that crack-bluntening can still arise by some localized plastic deformation process.   As the specimens are tested slowly at temperatures as much as 80° below Tg, it is unlikely that thermal effects are significant (if compared with data for PMMA by Kambour [28]).

It is highly likely that environmental crazing is occurring in these experiments, as the phenomena is now well documented for these [29,30] and related amorphous polymers [31-34].   For polydienes, conditions for crazing are pre-orientation, low strain rates and test temperatures near the liquification temperature of the environment [30].   More recently it was shown [29] that pre-oriented peroxy-crosslinked polybutadiene when strained at 93°K in nitrogen led to prolific, prominent crazing.   However when the pre-extension (normally 100-300%) was not undertaken, brittle behaviour was noted with no craze formation.   When nitrogen was replaced by helium, no crazing was noted, agreeing with related studies using other polymers [36].   During crazing, large amounts of gas are absorbed, although the hypothesis that storage is in craze voids has not been directly substantiated.

In the double torsion testing, conditions are similar to those described by Mead et al [29], except that no intended pre-extension exists (and residual orientation caused by milling and other sample preparation steps would appear to be no greater than in their experiments), and double torsion test geometry is rather more complex than simple uniaxial tensile testing.   In several experiments, the test pieces

were coated with a silicone grease to try to retard nitrogen penetration, but similar results as for uncoated samples were obtained.

Despite these aforementioned experimental differences, it is most likely that the predominant contributor to high fracture energy is environmental crazing. With the absence of pre-orientation the extent of crazing is not expected to be as great as indicated by Mead [29], so that the rubber will be sufficiently embrittled for double-torsion fracture energy measurement to be of some value.

4.2.2 Sulphur-cured polybutadiene

The extremes in practical levels of sulphur are generally from 1 to 2 parts, and this corresponds to a rather narrow range of crosslink densities (i.e. M_c from 3,200 to 4,900). Fracture energies are provided for three compounds tested at three crosshead speeds (Fig. 9). Ignoring the suspect high speed data, it will be noted that G_{Ic} ranges from a little over 5 kJM^{-2} to perhaps about 10 kJM^{-2}. However, as for the peroxide cured samples, no great sensitivity to crosslink density was again observed. It is considered that at the maximum crosslink density employed, crazing or other crack bluntening modes of deformation are possible. The use of unusually high levels of sulphur to reduce M_c to below 1000 may cause a change in mode of failure although this step would be of limited practical importance. For environmental crazing, the rate of uptake of nitrogen is undiminished and little change in G_{Ic} is expected.

Strain rate effects for this set of polymers were more pronounced than for the peroxide-cured polymer (Fig. 10). The reason for this departure is not clear.

4.3   Morphology of polymer fracture surfaces.

As it was known that liquid nitrogen environmental crazing had already been reported for similar polymers [29,30] and as fracture energy values obtained were higher than for many brittle linear polymers, the test pieces were examined closely during and after double torsion tensile testing.

Some circumstantial evidence for nitrogen penetration in cis-polybutadiene was that the bulk material changed from transparent bright yellow to a more opaque cream colour upon chilling. This change was reversible, with the exterior recovering first. The cross-section was similar to that shown for polychloroprene (Fig. 6, [29]).

Fracture surfaces (Fig. 11) macroscopically resemble familiar mirror-like craze texture observed in PMMA and polystyrene. This pearl-like or opalescent appearance is caused by the differing refractive index of the essentially spongelike matter compared with the homogeneous uncrazed bulk [37,38].

When specimens are brought to 20°C, this characteristic craze sheen is lost, and macroscopically all that can be seen are the characteristic double torsion fracture zones (Fig. 12) which correspond to the description by Hakeem and Phillips [13] for PMMA. At higher magnification no evidence for craze material can be detected (Fig. 13), although this is hardly surprising, as fine oriented remnants will have disappeared during the 200°C increase in temperature. The retention of low temperature structure for the purposes of high resolution microscopy constitutes a major and presently practical challenge.

5. Conclusions

Crosslinked rubbers with no pre-orientation can be tested by the double torsion method and estimates of fracture energy obtained. Under slow strain rate conditions stable crack propagation transpired, and.fracture energy values of about 5 kJM^{-2} were recorded. This high value was rather insensitive to both strain rate, crosslink density and type. The major cause for high toughness is considered to be liquid nitrogen environmental crazing, although direct high resolution morphological data is lacking. Further double torsion studies where inert helium is substituted for nitrogen as the coolant, will be undertaken to establish the contribution made to fracture energy by the environment.

REFERENCES

1. R.P. Burford, Conservation and Recycling, 4 (4), (1981) 219.

2. R. Schaub, Gummi. Asbest. Kunststoffe, 31 (6), (1978) 404.

3. I.B. Mishra, J.A. Koutsky and N.R. Braton, Polymer News, 2 (9,10), (1976) 32.

4. H.H. Kausch, 'Polymer Fracture' (Springer-Verlag, Berlin Heidelberg, 1978), 260.

5. A. Ahagon and A.N. Gent, J. Polym. Sci., Polym. Phys. Ed., 13, (1975) 1903.

6. G. J. Lake, P.B. Lindley and A.G. Thomas, Proceedings of the Second Int. Conf. on Fracture, Brighton 1969, edited by P.L. Pratt (Chapman and Hall Ltd., London, 1969) Paper 43, p.493.

7. F.A. Johnson and J.C. Radon, J. Polym. Sci., Polym. Chem. Ed., 11, (1973) 1995.

8. G.P. Marshall, L.H. Coutts and J.G. Williams, J. Materials Sci., 9, (1974) 1409.

9. J.A. Kies and A. J. Clark, Proceedings of the Second Int. Conf. on Fracture, Brighton, 1969, Edited by P.L. Pratt (Chapman and Hall Ltd., London, 1969), Paper 42, p. 483.

10. D.P. Williams and A.G. Evans, J. Testing Evaluation, 1 (4), (1973) 264.

11. A.G. Evans, J. Mater. Sci., 7 (1972), 1137.

12. P.W. Beaumont and R.J. Young, J. Mater. Sci., 10 (1975), 1334.

13. M.I. Hakeem, M.G. Phillips, J. Mater. Sci., 14 (1979) 2901.

14. M. Parvin and J.G. Williams, J. Mater. Sci., 10 (1975) 1883.

15. J.O. Outwater and D.J. Gerry, J. Adhesion, 1 (1969) 290.

16. R.A. Glendhill, A.J. Kinloch, S. Yamini and R.J. Young, Polymer, 19 (1978) 574.

17. S. Yamini and R.J. Young, Polymer, 18 (1977) 1075.

18. S. Yamini and R.J. Young, J. Mater. Sci., 15 (1980) 1823.

19. J.M. Scott, G.M. Wells and D.C. Phillips, J. Mater. Sci., 15 (1980), 1436.

20. D.C. Phillips, J.M. Scott and M.Jones, J. Mater. Sci., 13 (1978) 311.

21. A. de S. Jayatilaka, 'Fracture of Engineering Brittle Materials', (Applied Science Publisher, London, 1979).

22. Phillips Petroleum Co. product information.

23. P.J. Flory and J. Rehner, Jr., J. Chem. Phys., 11 (1943) 521. P.J. Flory, ibid. 18, (1950) 108.

24. G. Kraus, J. Appl. Polym. Sci., 7 (1963), 1257.

25. A. N. Gent and A. W. Henry, Proc. Int. Rubber Conf., (1967), 193.

26. J. G. Williams, 'Applications of Linear Fracture Mechanics', in "Failure in Polymers" (Advances in Polymer Science, Vol. 27, Springer-Verlag, Berlin, Heidelberg, 1978), p.80.

27. J.G. Williams and J.M. Hodgkinson, Proc. R.Soc. Lond. A, 375 (1981) 231.

28. R.P. Kambour and R.E. Barker Jr., J. Polym. Sci., A.2, 4 (1966) 359.

29. W.T. Mead, R.S. Porter and P.E. Reed, J. Materials Sci., 14 (1979) 850.

30. W.T. Mead and P.E. Reed, Polymer Eng. and Sci., 14 (1974) 22.

31. H.G. Olf and A. Peterlin, J. Polym. Sci., Polym. Phys. Ed., 12 (1974) 2209.

32. M.F. Parrish and N. Brown, Nature, 237 (1972) 122.

33. N. Brown and B.D. Metzger, J. Appl. Phys., 48 (1977) 4109.

34. R.D. Brown, K.L. DeVries and M.L. Williams, in"Polymer Networks: Structural and Mechanical Properties", ed. N.J. Chompff, Plenum Press, New York, 1971.

35. Y. Imai and N. Brown, J. Polym. Sci., Polym. Phys. Ed., 14, (1976) 723.

36. N. Brown and Y. Imai, J. Polym. Sci., B13 (1975) 511.

37. R.P. Kambour, J.Polym. Sci., A2 (1964) 4159.

38. B.L. Earl, R.J. Loneragan, J. Markham and M. Crook, J. Appl. Polym. Sci., 18 (1974) 245.

Figure 1.   Double torsion test apparatus.

Figure 2.   Load versus deflection trace.

Figure 3.   Evenly spaced crack arrest lines on fracture surface
of peroxide-crosslinked polybutadiene.

Figure 4.   Fracture energy G_{I_C} versus strain rate, for PMMA.

Figure 5.   Slip-stick trace for cis-BR with 1 phr sulphur,
crosshead speed 0.5 mm min^{-1}.

Figure 6.   Load versus deflection trace showing more continuous
crack propagation (1.5 phr sulphur, crosshead speed
0.5 mm min^{-1}).

Figure 7.   Load versus deflection trace - unstable crack growth
at high crosshead speeds.

Figure 8.   Effect of crosslink density upon G_{I_C}, peroxide cured
polybutadiene.

Figure 9.   Fracture energy versus crosshead speed: sulphur-cured
polybutadiene $\triangle$ = 1.0 phr, $\bigtriangledown$ = 1.5 phr, 0 = 2.0 phr.

Figure 10.   Effect of strain rate upon fracture energy peroxide-
cured polybutadienes, $\triangle$ = 0.05, 0 = 0.2, ■ = 0.4, ● = 0.6 phr.

Figure 11.   Low magnification fracture morphology of peroxide-
crosslinked polybutadiene, in cold nitrogen atmosphere.

Figure 12.   Fracture zones of broken double torsion specimens
peroxide-cured polybutadiene.

Figure 13.   Scanning electron micrograph of fractured double torsion
specimen at 20°C.

TO INSTRON CROSSHEAD

N₂

INSULATION

LOAD CELL

Figure 1

TIME ∝ DEFLECTION

Figure 2

Figure 3

CROSSHEAD SPEED (mm min^{-1})

Figure 4

STABLE REGION

UNSTABLE REGION
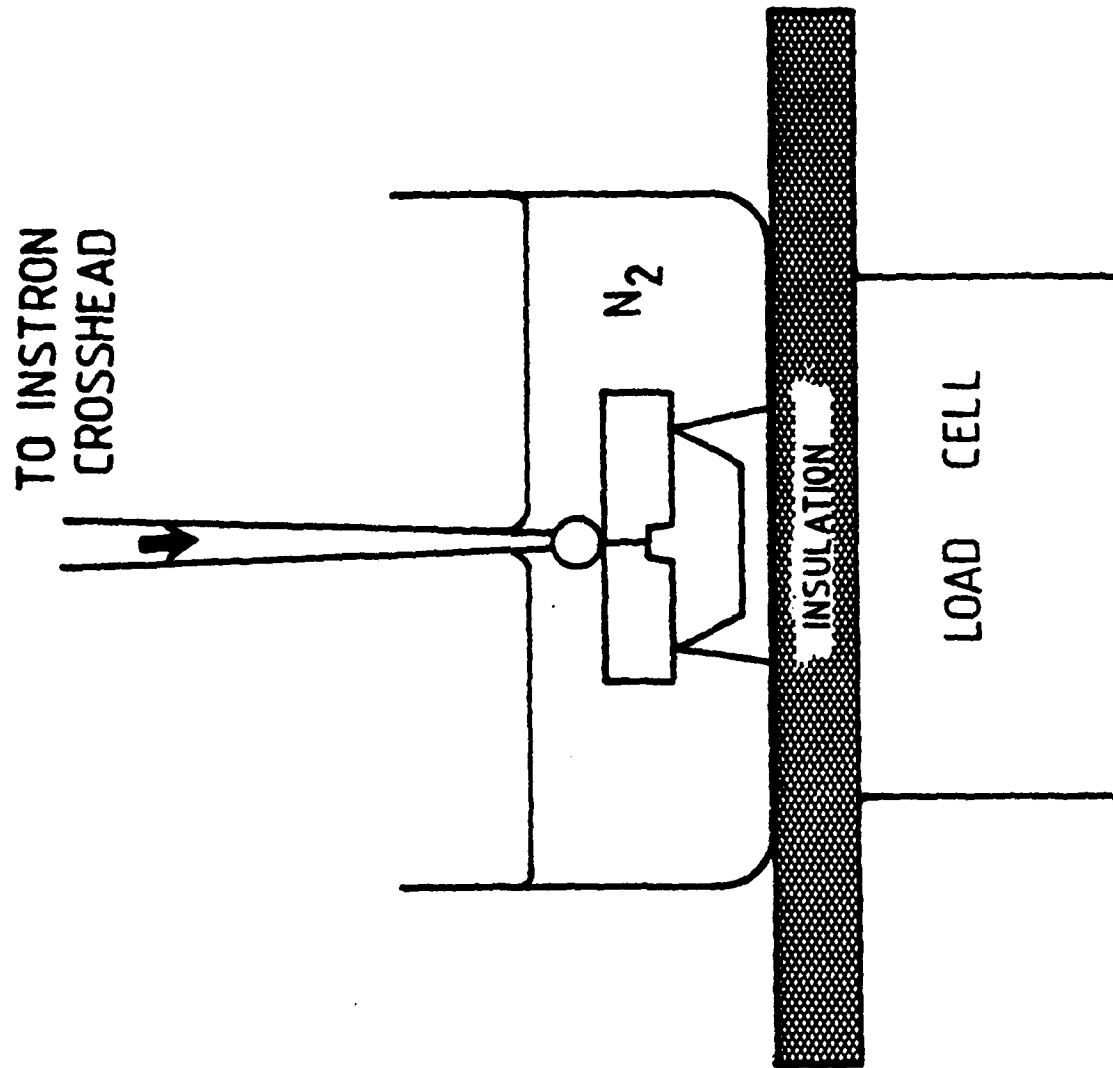
LOAD (N)
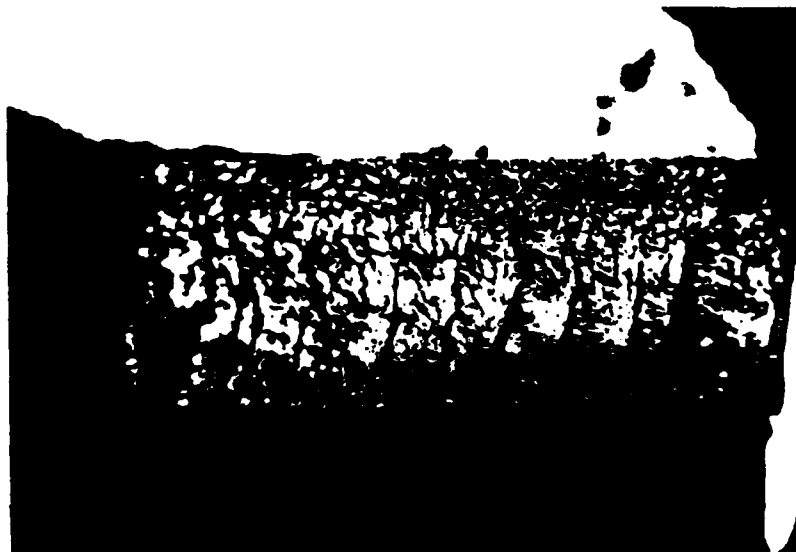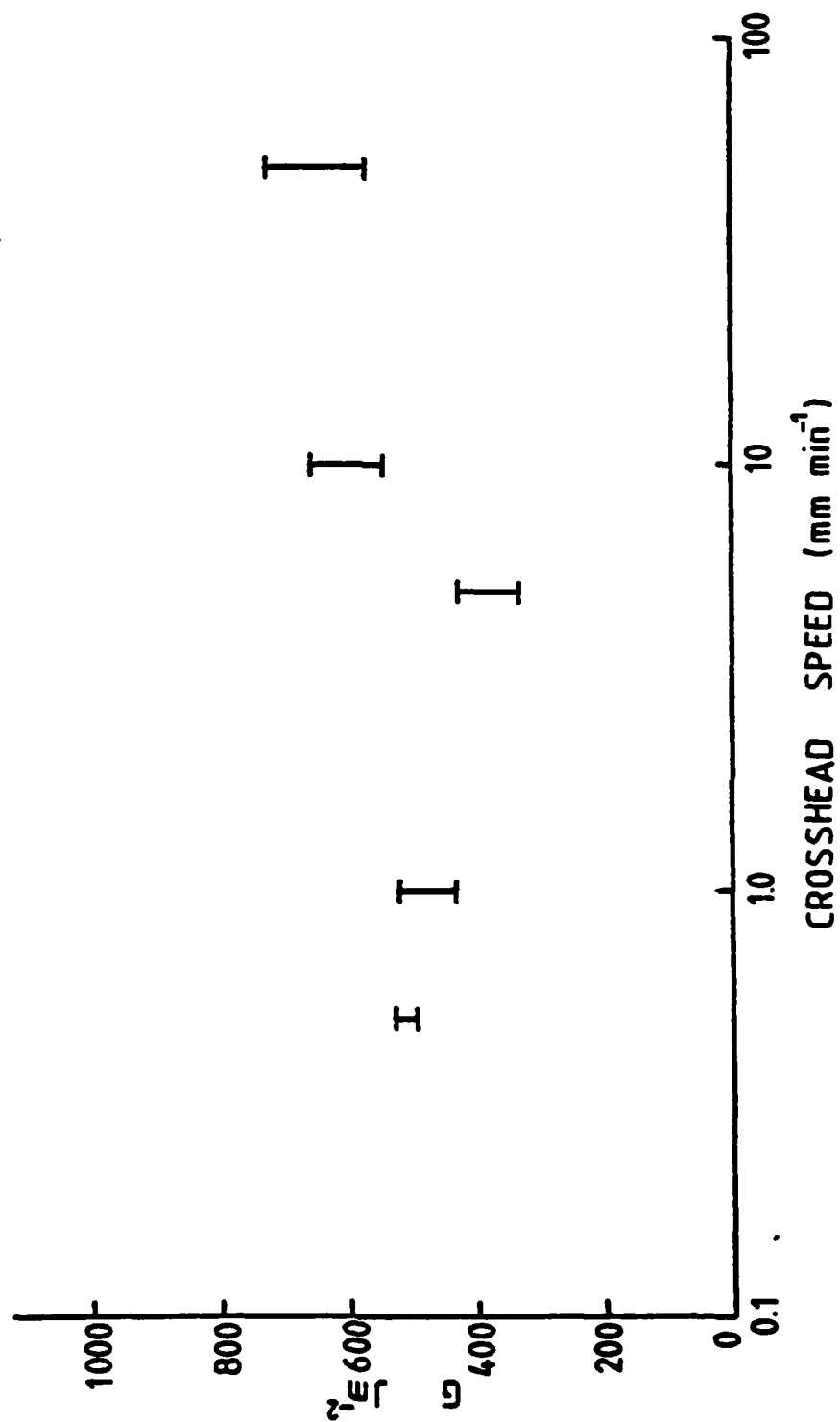
TIME ∝ DEFLECTION

Figure 5

TIME ∝ DEFLECTION

Figure 6

Figure 7

LOG Mc
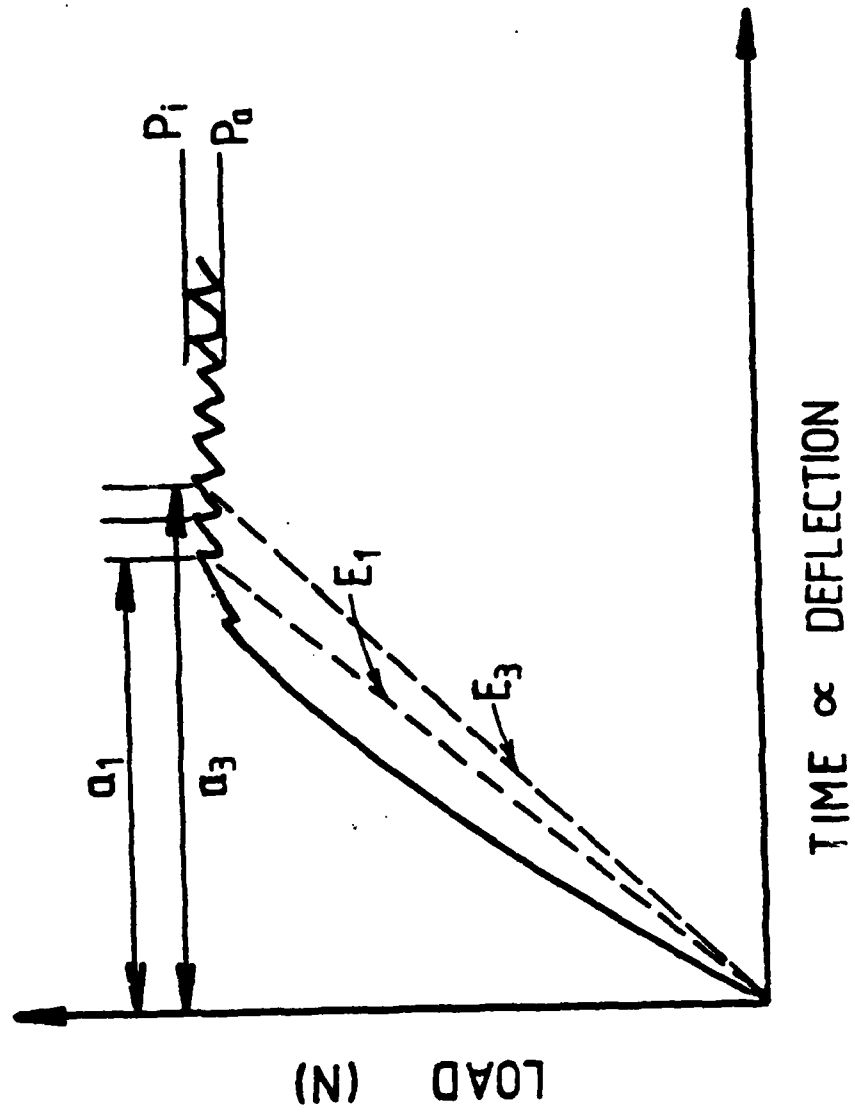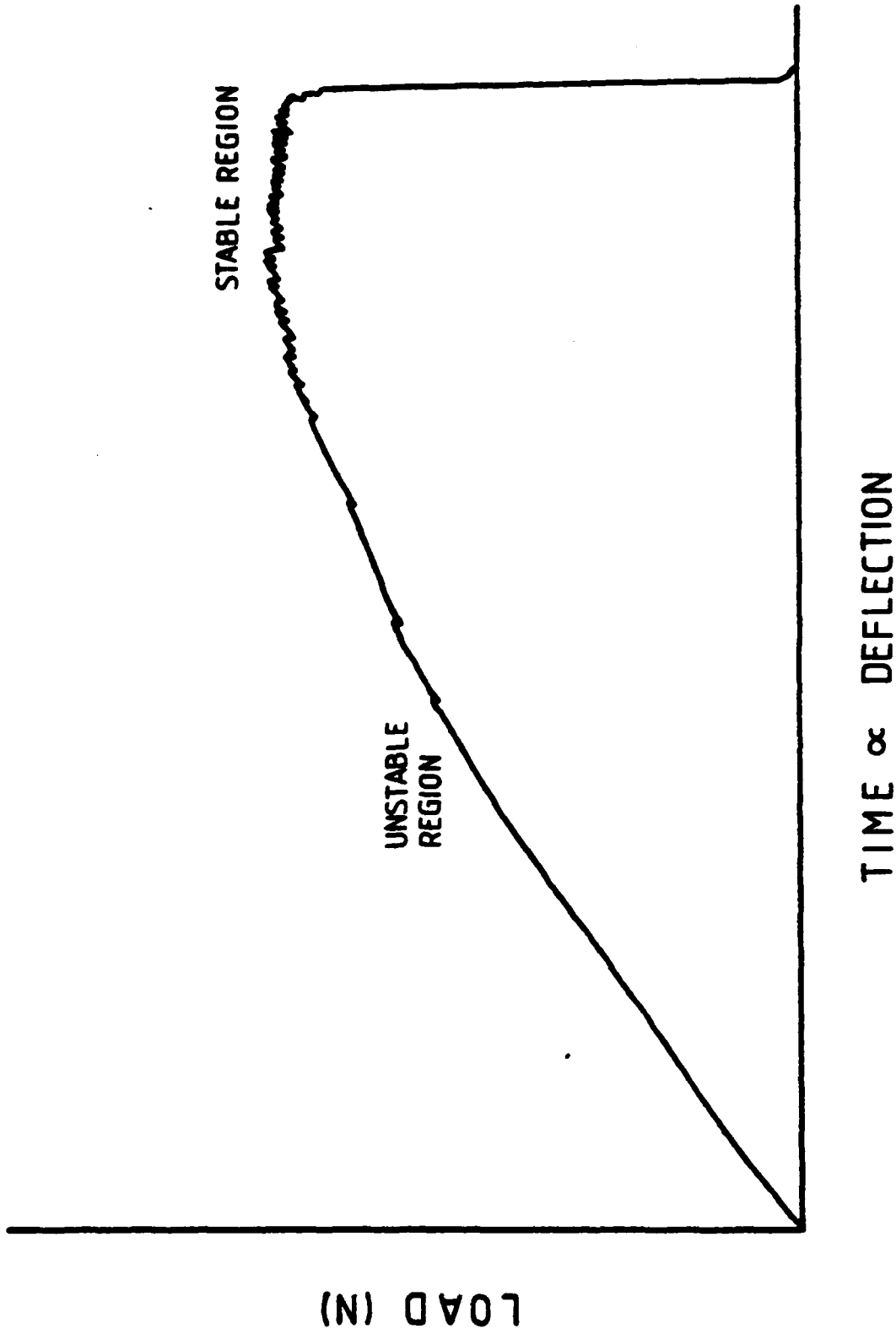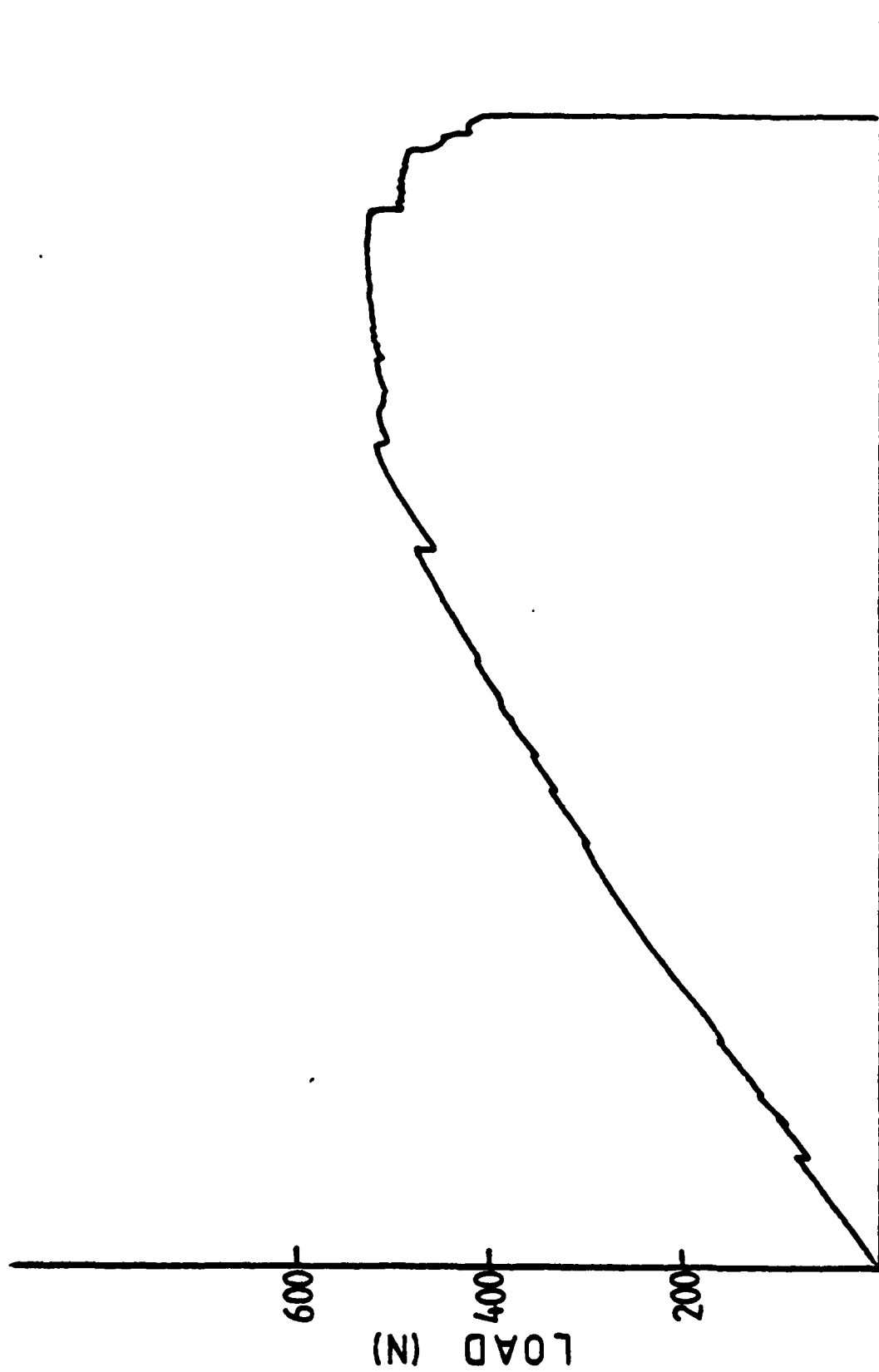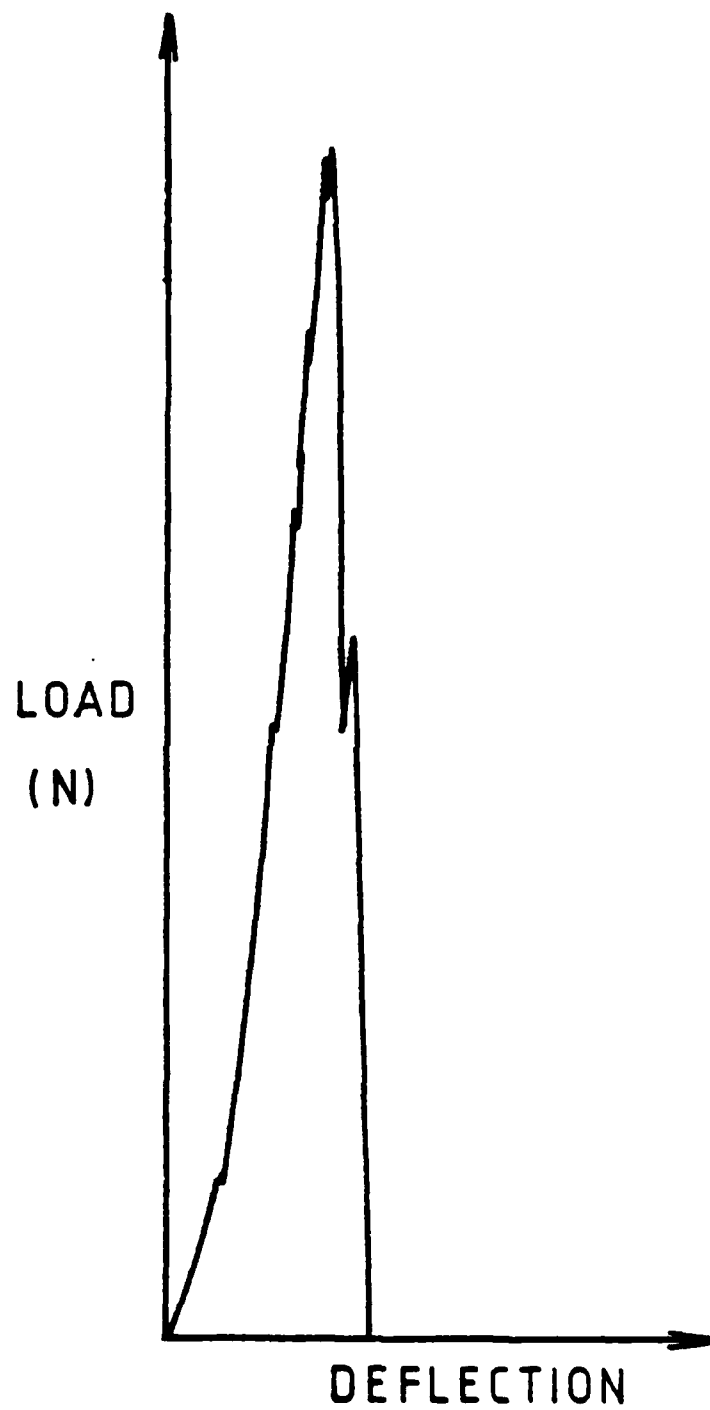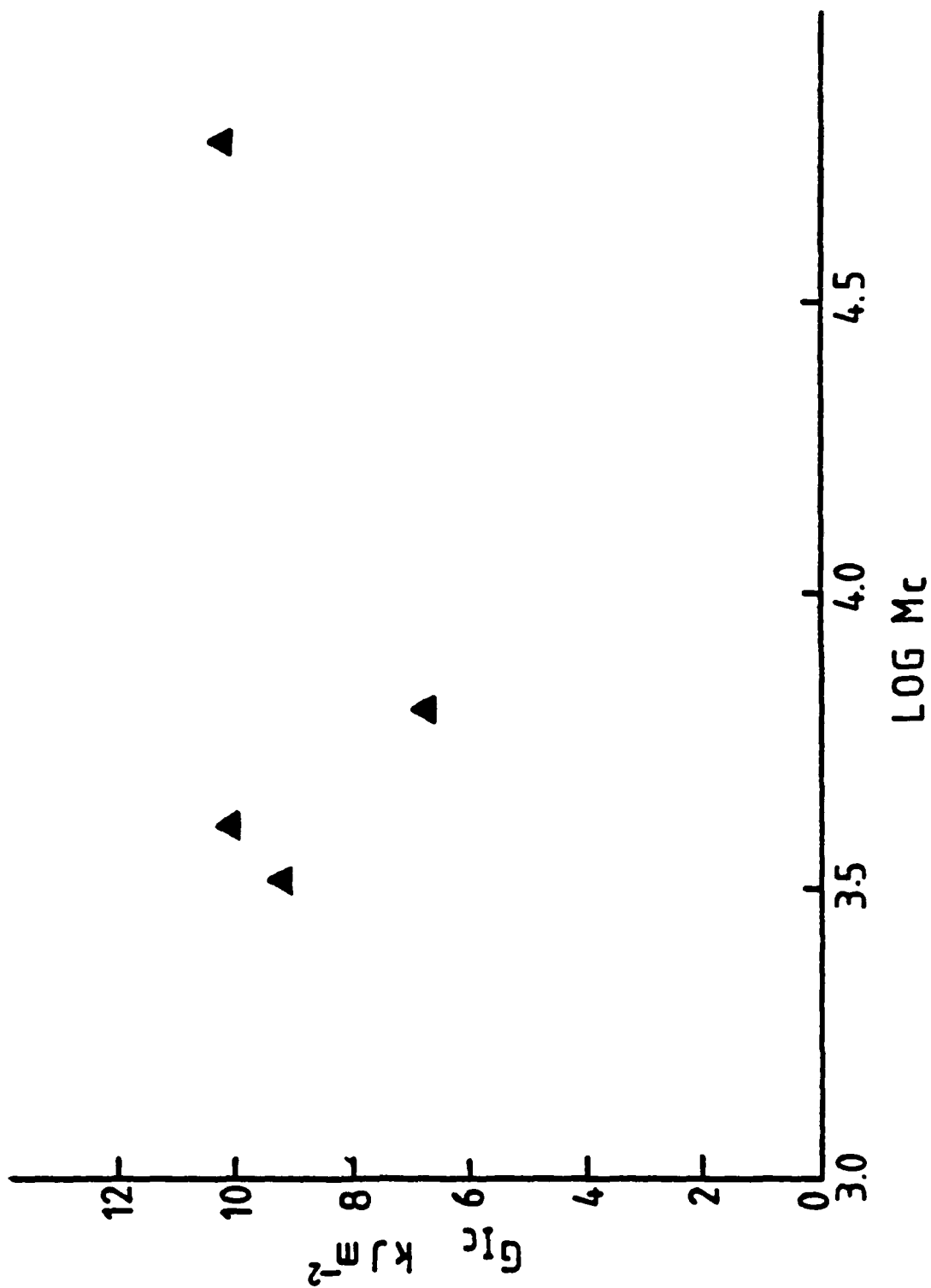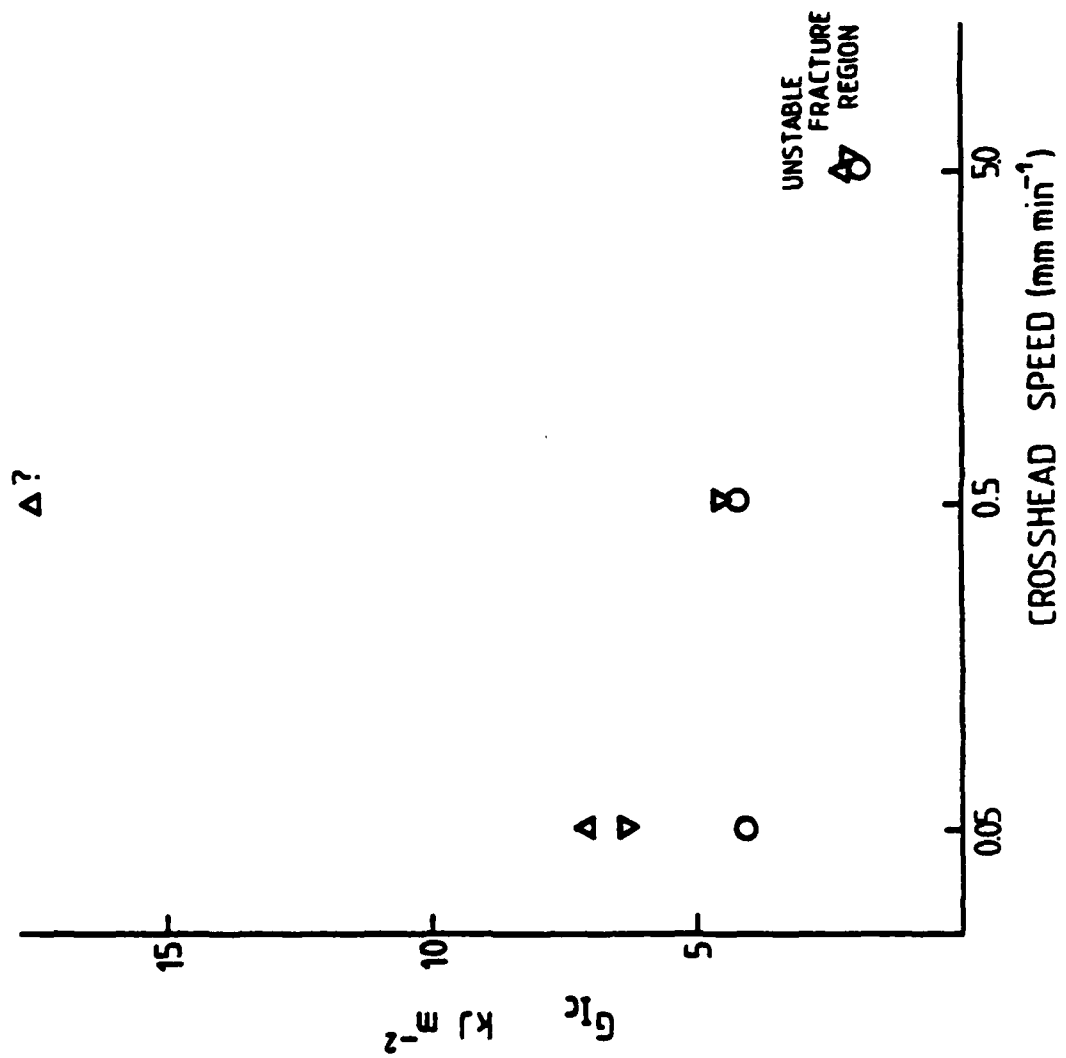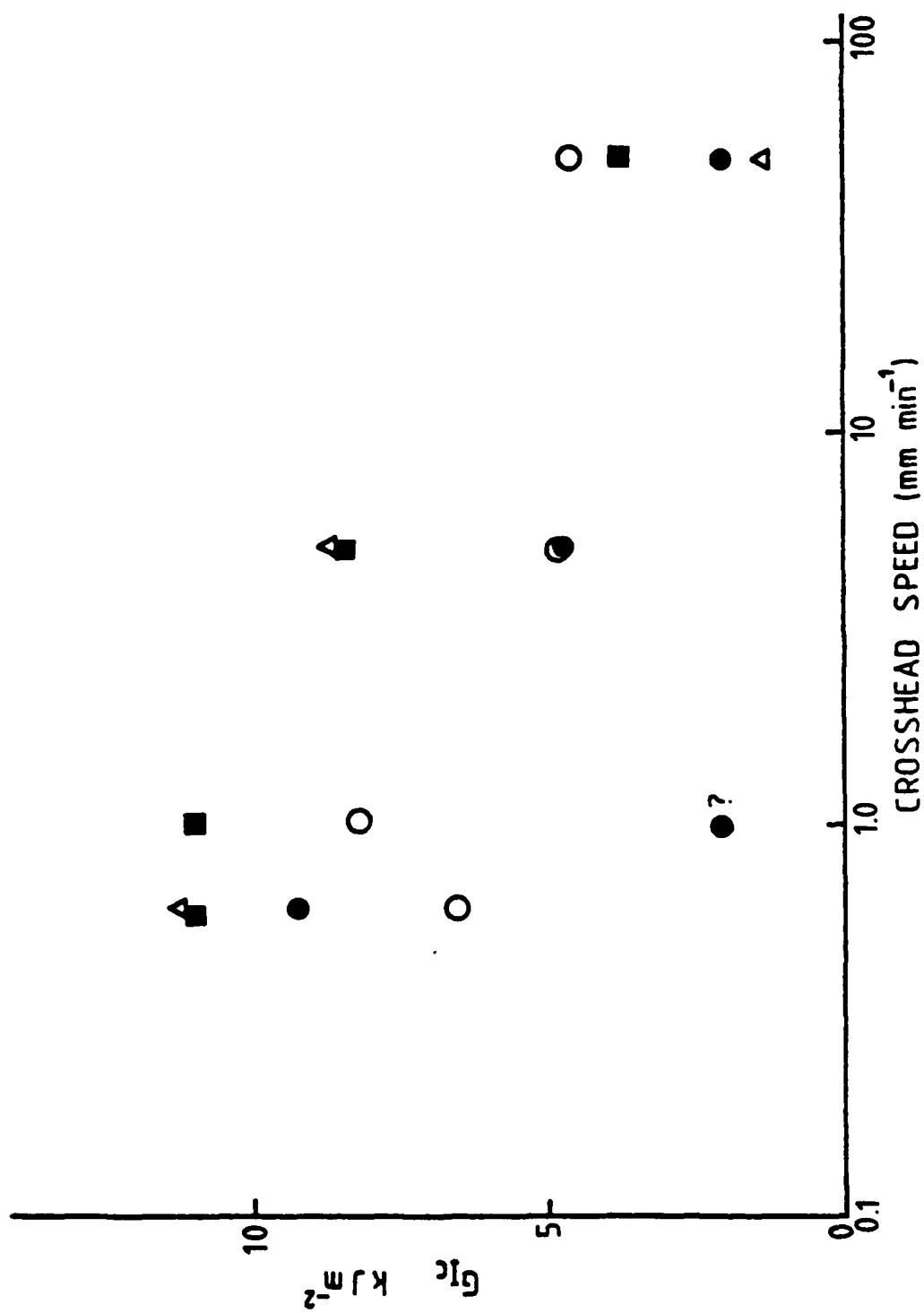
Figure 8

Figure 9

Figure 10

Figure 11

Figure 12
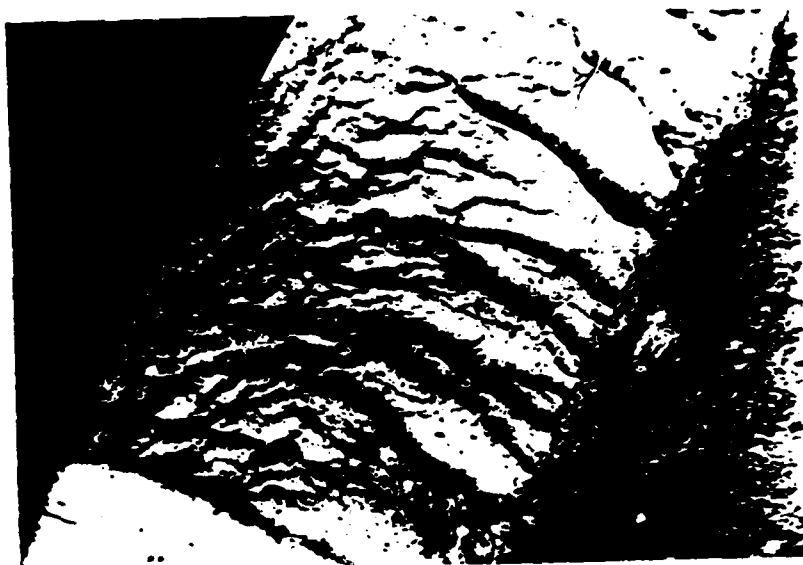
Figure 13

DISTRIBUTION LIST

	No. Copies		No. Copies
Dr. L.V. Schmidt Assistant Secretary of the Navy (R,E, and S) Room 5E 731 Pentagon Washington, D.C. 20350	1	Dr. F. Roberto Code AFRPL MKPA Edwards AFB, CA 93523	1
Dr. A.L. Slafkosky Scientific Advisor Commandant of the Marine Corps Code RD-1 Washington, D.C. 20380	1	Dr. L.H. Caveny Air Force Office of Scientific Research Directorate of Aerospace Sciences Bolling Air Force Base Washington, D.C. 20332	1
Dr. Richard S. Miller Office of Naval Research Code 413 Arlington, VA 22217	10	Mr. Donald L. Ball Air Force Office of Scientific Research Directorate of Chemical Sciences Bolling Air Force Base Washington, D.C. 20332	1
Mr. David Siegel Office of Naval Research Code 260 Arlington, VA 22217	1	Dr. John S. Wilkes, Jr. FJSRL/NC USAF Academy, CO 80840	1
Dr. R.J. Marcus Office of Naval Research Western Office 1030 East Green Street Pasadena, CA 91106	1	Dr. R.L. Lou Aerojet Strategic Propulsion Co. P.O. Box 15699C Sacramento, CA 95813	1
Dr. Larry Peebles Office of Naval Research East Central Regional Office 666 Summer Street, Bldg. 114-D Boston, MA 02210	1	Dr. V.J. Keenan Anal-Syn Lab Inc. P.O. Box 547 Paoli, PA 19301	1
Dr. Phillip A. Miller Office of Naval Research San Francisco Area Office One Hallidie Plaza, Suite 601 San Francisco, CA 94102	1	Dr. Philip Howe Army Ballistic Research Labs ARRADCOM Code DRDAR-BLT Aberdeen Proving Ground, MD 21005	1
Mr. Otto K. Heiney AFATL - DLDL Elgin AFB, FL 32542	1	Mr. L.A. Watermeier Army Ballistic Research Labs ARRADCOM Code DRDAR-BLI Aberdeen Proving Ground, MD 21005	1
Mr. R. Geisler ATTN: MKP/MS24 AFRPL Edwards AFB, CA 93523	1	Dr. W.W. Wharton Attn: DRSMI-RKL Commander U.S. Army Missile Command Redstone Arsenal, AL 35898	1

DISTRIBUTION LIST

	No. Copies		No. Copies
Dr. R.G. Rhoades Commander Army Missile Command DRSMI-R Redstone Arsenal, AL 35898	1	Dr. E.H. Debutts Hercules Inc. Baccus Works P.O. Box 98 Magna, UT 84044	1
Dr. W.D. Stephens Atlantic Research Corp. Pine Ridge Plant 7511 Wellington Rd. Gainesville, VA 22065	1	Dr. James H. Thacher Hercules Inc. Magna Baccus Works P.O. Box 98 Magna, UT 84044	1
Dr. A.W. Barrows Ballistic Research Laboratory USA ARRADCOM DRDAR-BLP Aberdeen Proving Ground, MD 21005	1	Mr. Theordore M. Gilliland Johns Hopkins University APL Chemical Propulsion Info. Agency Johns Hopkins Road Laurel, MD 20810	1
Dr. C.M. Frey Chemical Systems Division P.O. Box 358 Sunnyvale, CA 94086	1	Dr. R. McGuire Lawrence Livermore Laboratory University of California Code L-324 Livermore, CA 94550	1
Professor F. Rodriguez Cornell University School of Chemical Engineering Olin Hall, Ithaca, N.Y. 14853	1	Dr. Jack Linsk Lockheed Missiles & Space Co. P.O. Box 504 Code Org. 83-10, Bldg. 154 Sunnyvale, CA 94088	1
Defense Technical Information Center DTIC-DDA-2 Cameron Station Alexandria, VA 22314	12	Dr. B.G. Craig Los Alamos National Lab P.O. Box 1663 NSP/DOD, MS-245 Los Alamos, NM 87545	1
Dr. Rocco C. Musso Hercules Aerospace Division Hercules Incorporated Alleghany Ballistic Lab P.O. Box 210 Washington, D.C. 21502	1	Dr. R.L. Rabie WX-2, MS-952 Los Alamos National Lab. P.O. Box 1663 Los Alamos NM 37545	1
Dr. Ronald L. Simmons Hercules Inc. Eglin AFATL/DLDL Eglin AFB, FL 32542	1	Dr. R. Rogers WX-2 Los Alamos Scientific Lab. P.O. Box 1663 Los Alamos, NM 87545	1

DISTRIBUTION LIST

	No. Copies		No. Copies
Mr. R. Brown Naval Air Systems Command Code 330 Washington, D.C. 20361	1	Dr. J. Schnur Naval Research Lab. Code 6510 Washington, D.C. 20375	1
Dr. H. Rosenwasser Naval Air Systems Command AIR-310C Washington, D.C. 20360	1	Mr. R. Beauregard Naval Sea Systems Command SEA 64E Washington, D.C. 20352	1
Mr. B. Sobers Naval Air Systems Command Code 03P25 Washington, D.C. 20360	1	Mr. G. Edwards Naval Sea Systems Command Code 62R3 Washington, D.C. 20362	1
Dr. L.R. Rothstein Assistant Director Naval Explosives Dev. Engineering Dept. Naval Weapons Station Yorktown, VA 23691	1	Mr. John Boyle Materials Branch Naval Ship Engineering Center Philadelphia, PA 19112	1
Dr. Lionel Dickinson Naval Explosive Ordnance Disposal Tech. Center Code D Indian Head, MD 20640	1	Dr. H.G. Adolph Naval Surface Weapons Center Code R11 White Oak Silver Spring, MD 20910	1
Mr. C.L. Adams Naval Ordnance Station Code PM4 Indian Head, MD 20640	1	Dr. T.D. Austin Naval Surface Weapons Center Code R16 Indian Head, MD 20640	1
Mr. S. Mitchell Naval Ordnance Station Code 5253 Indian Head, MD 20640	1	Dr. T. Hall Code R-11 Naval Surface Weapons Center White Oak Laboratory Silver Spring, MD 20910	1
Dr. William Tolles Dean of Research Naval Postgraduate School Monterey, CA 93940	1	Mr. G.L. Mackenzie Naval Surface Weapons Center Code R101 Indian Head, MD 20640	1
Naval Research Lab. Code 6100 Washington, D.C. 20375	1	Dr. K.F. Mueller Naval Surface Weapons Center Code R11 White Oak Silver Spring, MD 20910	1

DISTRIBUTION LIST

No. Copies		No. Copies	
Mr. J. Murrin Naval Sea Systems Command Code 62R2 Washington, D.C. 20362	1	Dr. A. Nielsen Naval Weapons Center Code 385 China Lake, CA 93555	1
Dr. D.J. Pastine Naval Surface Weapons Cneter Code R04 White Oak Silver Spring, MD 20910	1	Dr. R. Reed, Jr. Naval Weapons Center Code 388 China Lake, CA 93555	1
Mr. L. Roslund Naval Surface Weapons Center Code R122 White Oak, Silver Spring MD 20910	1	Dr. L. Smith Naval Weapons Center Code 3205 China Lake, CA 93555	1
Mr. M. Stosz Naval Surface Weapons Center Code R121 White Oak Silver Spring, MD 20910	1	Dr. B. Douda Naval Weapons Support Center Code 5042 Crane, Indiana 47522	1
Dr. E. Zimmet Naval Surface Weapons Center Code R13 White Oak Silver Spring, MD 20910	1	Dr. A. Faulstich Chief of Naval Technology MAT Code 0716 Washington, D.C. 20360	1
Dr. D. R. Derr Naval Weapons Center Code 388 China Lake, CA 93555	1	LCDR J. Walker Chief of Naval Material Office of Naval Technology MAT, Code 0712 Washington, D.C. 20360	1
Mr. Lee N. Gilbert Naval Weapons Center Code 3205 China Lake, CA 93555	1	Mr. Joe McCartney Naval Ocean Systems Center San Diego, CA 92152	1
Dr. E. Martin Naval Weapons Center Code 3858 China Lake, CA 93555	1	Dr. S. Yamamoto Marine Sciences Division Naval Ocean Systems Center San Diego, CA 91232	1
Mr. R. McCarten Naval Weapons Center Code 3272 China Lake, CA 93555	1	Dr. G. Bosmajian Applied Chemistry Division Naval Ship Research & Development Center Annapolis, MD 21401	1
		Dr. H. Shuey Rohn and Haas Company Huntsville, Alabama 35801	1

DISTRIBUTION LIST

No. Copies   No. Copies

                                              1
Dr. J.F. Kincaid   1   Dr. C.W. Vriesen
Strategic Systems Project   Thiokol Elkton Division
Office   P.O. Box 241
Department of the Navy   Elkton, MD 21921
Room 901
Washington, D.C. 20376   Dr. J.C. Hinshaw   1
                                              Thiokol Wasatch Division
                                              P.O. Box 524
Strategic Systems Project Office   1   Brigham City, Utah 84302
Propulsion Unit
Code SP2731   U.S. Army Research Office   1
Department of the Navy   Chemical & Biological Sciences
Washington, D.C. 20376   Division
                                              P.O. Box 12211
Mr. E.L. Throckmorton   1   Research Triangle Park
Strategic Systems Project Office   NC 27709
Department of the Navy
Room 1048   Dr. R.F. Walker   1
Washington, D.C. 20376   USA ARRADCOM
                                              DRDAR-LCE
Dr. D.A. Flanigan   1   Dover, NJ 07001
Thiokol
Huntsville Division   Dr. T. Sinden   1
Huntsville, Alabama   35807   Munitions Directorate
                                              Propellants and Explosives
                                              Defence Equipment Staff
Mr. G.F. Mangum   1   British Embassy
Thiokol Corporation   3100 Massachusetts Ave.
Huntsville Division   Washington, D.C. 20003
Huntsville, Alabama   35807
                                              LTC B. Loving   1
Mr. E.S. Sutton   1   AFROL/LK
Thiokol Corporation   Edwards AFB, CA 93523
Elkton Division
P.O. Box 241   Professor Alan N. Gent   1
Elkton, MD 21921   Institute of Polymer Science
                                              University of Akron
Dr. G. Thompson   1   Akron, OH 44325
Thiokol
Wasatch Division   Mr. J. M. Frankle   1
MS 240 P.O. Box 524   Army Ballistic Research Labs
Brigham City, UT 84302   ARRADCOM
                                              Code DRDAR-BLI
Dr. T.F. Davidson   1   Aberdeen Proving Ground, MD 21005
Technical Director
Thiokol Corporation
Government Systems Group
P.O. Box 9253
Odgen, Utah 84409

DISTRIBUTION LIST

No. Copies

Dr. Ingo W. May Army Ballistic Research Labs ARRADCOM Code DRDAR-BLI Aberdeen Proving Ground, MD 21005	1

Dr. J. P. Marshall Dept. 52-35, Bldg. 204/2 Lockheed Missile & Space Co. 3251 Hanover Street Palo Alto, CA 94304	1

Professor N.W. Tschoegl   1
California Institute of Tech
Dept. of Chemical Engineering
Pasadena, CA 91125

Ms. Joan L. Janney   1
Los Alamos National Lab
Mail Stop 920
Los Alamos, NM 87545

Professor M.D. Nicol   1
University of California
Dept. of Chemistry
405 Hilgard Avenue
Los Angeles, CA 90024

Dr. J. M. Walsh   1
Los Alamos Scientific Lab
Los Alamos, NM 87545

Professor R. W. Armstrong   1
Univ. of Maryland
Department of Mechanical Eng.
College Park, MD 20742

Professor A. G. Evans   1
University of California
Berkeley, CA 94720

Prof. Richard A. Reinhardt   1
Naval Postgraduate School
Physics & Chemistry Dept.
Monterey, CA 93940

Professor T. Litovitz   1
Catholic Univ. of America
Physics Department
520 Michigan Ave., N.E.
Washington, D.C. 20017

Dr. R. Bernecker   1
Naval Surface Weapons Center
Code R13
White Oak, Silver Spring, MD 20910

Professor W. G. Knauss   1
Graduate Aeronautical Lab
California Institute of Tech.
Pasadena, CA 91125

Dr. M. J. Kamlet   1
Naval Surface Weapons Center
Code R11
White Oak, Silver Spring, MD 20910

Professor Edward Price   1
Georgia Institute of Tech.
School of Aerospace Engin.
Atlanta, Georgia 30332

Professor J. D. Achenbach   1
Northwestern University
Dept. of Civil Engineering
Evanston, IL 60201

Dr. Kenneth O. Hartman   1
Hercules Aerospace Division
Hercules Incorporated
P.O. Box 210
Cumberland, MD 21502

Dr. N. L. Basdekas   1
Office of Naval Research
Mechanics Program, Code 432
Arlington, VA 22217

Dr. Thor L. Smith   1
IBM Research Lab
D42.282
San Jose, CA 95193

Professor Kenneth Kuo   1
Pennsylvania State Univ.
Dept. of Mechanical Engineering
University Park, PA 16802

DISTRIBUTION LIST

	No. Copies		No. Copies

Dr. S. Sheffield   1
Sandia Laboratories
Division 2513
P.O. Box 5800
Albuquerque, NM 87185

Dr. M. Farber   1
Space Sciences, Inc.
135 Maple Avenue
Monrovia, CA 91016

Dr. Y. M. Gupta   1
SRI International
333 Ravenswood AVenue
Menlo Park, CA 94025

Mr. M. Hill   1
SRI International
333 Ravenswood Avenue
Menlo Park, CA 94025

Professor Richard A. Schapery   1
Texas A&M Univ.
Dept of Civil Engineering
College Station, TX 77843

Dr. Stephen Swanson   1
Univ. of Utah
Dept. of Mech. & Industrial
    Engineering
MEB 3008
Salt Lake City, UT 84112

Mr. J. D. Byrd   1
Thiokol Corp. Huntsville
Huntsville Div.
Huntsville, AL 35807

Professor G. D. Duvall   1
Washington State University
Dept. of Physics
Pullman, WA 99163

Prof. T. Dickinson   1
Washington State University
Dept. of Physics
Pullman, WA 99163